Understanding the Aeroacoustic Radiation Sources and Mechanism in High-Speed Jets

Dissertation

Presented in Partial Fulfillment of the Requirements for the Degree Doctor of Philosophy in the Graduate School of The Ohio State University

By

Michael Crawley, B.S.

Graduate Program in Department of Mechanical Engineering

The Ohio State University

2015

Dissertation Committee:

Mo Samimy, Advisor

Datta Gaitonde

James Gregory

Mei Zhuang

Abstract

Who reads a dissertation abstract?

This work is dedicated to Science ...

Acknowledgments

I should probably acknowledge someone here ...

Vita

September 10, 1986	Born - Plano, Texas
2009	B.S. Mechanical Engineering, University of Texas, Austin.
2009-present	Graduate Research Associate, The Ohio State University.

Publications

Research Publications

M. Crawley, C.-W. Kuo, and M. Samimy, "Identification of the Acoustic Response in the Irrotational Near-field of an Excited Subsonic Jet." submitted to *International Journal of Aeroacoustics*.

M. Crawley, R. Speth, D. V. Gaitonde, and M. Samimy, "A Study of the Noise Source Mechanisms in an Excited Mach 0.9 Jet - Complementary Experimental and Computational Analysis." AIAA Paper 2015-0736, *53rd AIAA Aerospace Sciences Meeting*.

M. Crawley, A. Sinha, and M. Samimy, "Near-field and Acoustic Far-field Response of a High-Speed Jet Forced with Plasma Actuators." *AIAA Journal*, expected 2015.

M. Crawley and M. Samimy, "Decomposition of the Near-Field Pressure in an Excited Subsonic Jet." AIAA Paper 2014-2342, *20th AIAA/CEAS Aeroacoustics Conference*.

M. Crawley, A. Sinha, and M. Samimy, "Near-field Pressure and Far-field Acoustic Response of Forced High-Speed Jets." AIAA Paper 2014-0527, *52nd AIAA Aerospace Sciences Meeting*.

M. Crawley, H. Alkandry, A. Sinha, and M. Samimy, "Correlation of Irrotational Near-Field Pressure and Far-Field Acoustic in Forced High-Speed Jets." AIAA Paper 2013-2188, *19th AIAA/CEAS Aeroacoustics Conference*.

H. Alkandry, **M. Crawley**, A. Sinha, M. Kearney-Fischer, and M. Samimy, "An Investigation of the Irrotational Near Field of an Excited High-Speed Jet." AIAA Paper 2013-0325, *51st AIAA Aerospace Sciences Meeting*.

M. Crawley, M. Kearney-Fischer, and M. Samimy, "Control of a Supersonic Rectangular Jet Using Plasma Actuators." AIAA Paper 2012-2211, *18th AIAA/CEAS Aeroacoustics Conference*.

Fields of Study

Major Field: Mechanical and Aerospace Engineering

Contents

List of Tables

Table **Page**

List of Figures

Figure **Page**

Chapter 1: Introduction

1.1 Motivation

The advent of the turbojet engine led to a transformation in both commercial and military aviation, allowing for much faster flight than previously possible with propellor-driven aircraft. However, the increased thrust of turbojets has come at great cost; significant acoustic radiation is generated by the rotating components (compressor, turbine, fan), by the combustion process, and ultimately by the free jet itself. On the commercial side, the escalating number of flights, encroachment of urban and residential areas near airports, and tightening of environmental regulations have combined to force airports to institute curfews, surcharges and flight path restrictions to combat noise pollution. For the military, hearing damage inflicted on nearby personnel (particularly flight deck crew on aircraft carriers) has necessitated the implementation of noise reduction concepts on tactical aircraft. During takeoff and landing, when acoustic radiation is most problematic to ground crew and surrounding urban and residential areas, the dominant noise source of the jet engine is the aeroacoustic radiation generated by the high velocity engine exhaust. This has spurred extensive research, spanning over six decades, into the acoustic source mechanism in high speed, high Reynolds number jets.

While progress has been made in the field of aeroacoustics, both experimentally [4–6] as well as theoretically [1], understanding of jet noise sources and their radiation mechanisms remains incomplete [2]. This is due to the large number of interrelated parameters (e.g. Reynolds number, temperature ratio, acoustic Mach number, nozzle geometry, et cetera) as well as the large disparity in the associated length and time scales of the turbulent phenomena and the radiated noise. Simulations of controlled free shear layers have suggested that there is significant potential for noise reduction, on the order of 11 dB in some cases [Wei 2006]. However, these simulations relied on non-physically defined actuation (that is, forcing was applied over a defined region by arbitrary energy, momentum, and body force terms), and a physical interpretation of the optimum forcing parameters was not immediately clear to the researchers. Current noise-mitigation technologies for free jets have largely been applied in an adhoc fashion, due to our incomplete understanding of the aeroacoustic sources. Fully realizing this maximum noise reduction potential will require a much more detailed understanding of the mechanism (or mechanisms) by which free jets radiate to the far-field.

It is generally agreed that the dominant noise sources are related to the large-scale turbulent structures present in the mixing layer of the jet. What remains to be determined is what aspects of the large-scale structure evolution and interactions are relevant to the noise generation process. Theoretical models of spatially- and temporally-modulated wavepackets have shown great promise in replicating the observed characteristics of the dominant far-field noise [Cavalieri/Jordan?]. However, direct experimental data linking this structure evolution to the acoustic emission is

still lacking. It is on this vein that the current work is focused. Until recently, experimental data acquisition techniques have been unable to capture the flow physics with enough fidelity (lacking in either spatial or temporal resolution) in order to accurately model the large-scale structures and aeroacoustic sources. By combining contemporary data acquisition methods (free-field microphones and non-time-resolved particle image velocimetry) with novel post-processing algorithms this work aims to directly link the relevant vortex dynamics of the large-scale structures to the acoustic emission events, and in the process identify a simplified aeroacoustic source mechanism.

1.2 Background

1.2.1 Flow Control

Controlling the development of the jet plume, and hence controlling the rate of mixing or intensity and characteristics of the emitted acoustic radiation, is a long running goal of the aeroacoustic community. Passive, permanent modifications to the nozzle have been shown to be quite adept at this task; some examples of these include tabs [citations] and chevrons [citations]. These work to generate counter-rotating streamwise vortices in the developing shear layer, which serve to substantially increase mixing between the core and coflow in the near-nozzle region and ultimately retard the growth of large-scale axisymmetric structures [citation].

Unfortunately, these passive modifications have associated penalties to the engine performance, in terms of added weight or reduced thrust. Due to the passive nature of the flow modification, these performance penalties are in effect over the entire duration of the flight regardless of whether or not the noise reduction is needed. To improve engine efficiency, active control techniques are desired, since they can

be activated when needed, such as during takeoff and landing, and deactivated when unneeded, such as after a commercial airliner reaches cruising altitude. Active control techniques, which seek to manipulate instabilities in the jet shear layer, have been extensively studied in low-speed, low-Reynolds number jets, the most common of which is acoustic drivers [citations]. However, as the speed and Reynolds number of the jet is increased (to match those in practical applications), so too does the required bandwidth and energy of the active drivers. Hence, acoustic or magneto-hydrodynamic drivers lose control authority in these regimes, and more powerful actuators are required.

The last decade has seen a rapid growth in the development of plasma actuators for use in high-speed flow control; though as of yet they have not progressed past the experimental phase. Localized arc filament plasma actuators (LAFPAs) are one such class of plasma actuator, which were developed by a collaboration between the Gas Dynamics and Turbulence Laboratory (GDTL) and the Non-Equilibrium Thermodynamics Laboratory (NETL) at the Ohio State University. LAFPAs can provide the high-amplitude and high-frequency excitation required for control of high Mach number and high Reynolds number jets [citations]. GDTL has used these actuators for noise mitigation and flow control in Mach 0.9 [citations], Mach 1.3 [citations] and Mach 1.65 [citations] jets (both heated and unheated). A review of the development of LAFPAs and their use in flow control and fluid phenomena research in high speed, high Reynolds number jets can be found in Samimy et al. [citation]. More recently, the diagnostic potential of LAFPAs for understanding jet flow phenomena has been explored. Excitation of instabilities in the flow by LAFPAs results in a definitive

spatio-temporal origin to which resulting phenomena can be referenced. The absolute temporal reference afforded by LAFPA excitation provides researchers the ability to investigate the growth, saturation, and decay of structures with high fidelity. An example of their diagnostic potential can be found in the work of Kearney-Fischer et al. [citation], which investigated Mach wave radiation from heated, high Mach number jets using schlieren imaging phase-locked to LAFPAs.

Unlike their passive counterparts (such as tabs or chevrons), or some other potential active flow control technologies (such as fluidic chevrons), LAFPAs control the shear layer development indirectly by exciting naturally occurring instabilities. The sharp velocity gradient in the jet shear layer gives rise to the inviscid Kelvin-Helmholtz instability [citation].

TO DO:

- shear layer / jet instabilities
- large-scale structures / energy cascade / wavepackets

1.2.2 Components of Jet Noise

A simplified model of the noise generation process in stationary free jets can be found in Fig. [INSERT FIGURE]. This model is based off of the work of Tam et al [4, 5], who observed that the far-field spectra could be represented as a combination of two similarity spectra based on polar angle of the observer, regardless of jet Mach number or temperature. At observer angles close to the jet downstream axis, the spectra exhibited a clearly defined spectral peak (F-spectrum), whereas at sideline or upstream angles the spectra were broadband (G-spectrum). From this observation the two-component acoustic source model was born: fine-scale turbulence, dominant

in the near-nozzle region, is responsible for the omni-directional acoustic radiation that dominates the sideline and upstream polar angles. On the other hand, the large-scale turbulent structures which exist further downstream produce the superdirective radiation that is readily apparent at aft polar angles.

Additional noise source mechanisms have been identified for supersonic jets. In imperfectly expanded jets, shock cells are produced in the jet. As turbulent structures pass through these waves, the sharp pressure gradients cause them to emit acoustic radiation. This is observed directly in the far-field as a broad-band amplification at high frequencies, referred to simply as broad-band shock-associated noise (BBSAN). In stationary or subsonic airframes this radiation can generate a feedback loop, whereby the noise travels upstream to the nozzle exit, excites the initial shear layer, and produces new structures at the same frequency. A high-amplitude, narrow-band tone (screech noise) is the end result of this feedback loop. Lastly, supersonically-convecting (relative to the ambient) large-scale structures (which exist in supersonic and heated jets) produce high-amplitude, strongly-directional acoustic radiation towards aft angles. This Mach wave radiation can be explained by a wavy-wall analogy (Tam again?). In the present work, the jet is unheated and subsonic; as such these noise sources are not present and therefore neglected throughout the rest of this work.

TO DO:

- Create simplified figure of free jet showing high frequency versus low frequency radiation (based off of Tam 2008)
- Explain Tam's "two-component" source model, with additional experimental evidence?

1.2.3 Acoustic Source Models

By rearranging the Navier-Stokes equations, Lighthill [3] was able to transform the governing equations for fluid dynamics into an inhomogeneous convected wave equation. In this acoustic analogy, the source term comprises Reynolds stress, shear stress, and density fluctuation terms (commonly referred to as *Lighthill's stress tensor*). As this formulation is exact (aside from the assumption of a constant sound speed), complete knowledge of the source field will yield an exact solution for the acoustic far field. In practical applications (e.g. high-speed, turbulent jets) however, the full source field cannot be measured using current experimental capabilities nor simulated with sufficient fidelity, thereby requiring certain simplifications.

Chapter 2: Experimental Methodology

2.1 Anechoic Chamber

All experiments were conducted at the GDTL within the Aerospace Research Center at the Ohio State University. Compressed, dried, and filtered air is supplied to the facility from two cylindrical storage tanks with a total capacity of 43 m^3 and maximum storage pressure of 16 MPa. The air may be routed through a storage heater (not used in this study), which allows the jet to operate with a stagnation temperature up to 500 C, before expanding through a nozzle and exhausting horizontally into an anechoic chamber. Opposite the nozzle, a collector accumulates the jet and entrained air and exhausts to the outdoors. A schematic of the anechoic chamber can be seen in Fig. 2.1. The dimensions of the chamber are 6.20 m wide by 5.59 m long and 3.36 m tall, with internal wedge-tip to wedge-tip dimensions of 5.14 m by 4.48 m and 2.53 m, respectively. The design of the chamber produces a cutoff frequency of 160 Hz, below the frequencies of interest for this study. A more detailed description of the GDTL anechoic chamber properties and validation has been given by [Hahn?].

For this study a converging, axisymmetric nozzle with exit diameter D of 25.4 mm was used. The internal contour of the nozzle was designed using a fifth order polynomial. The nozzle utilized a thick-lipped design in order to simplify the mounts

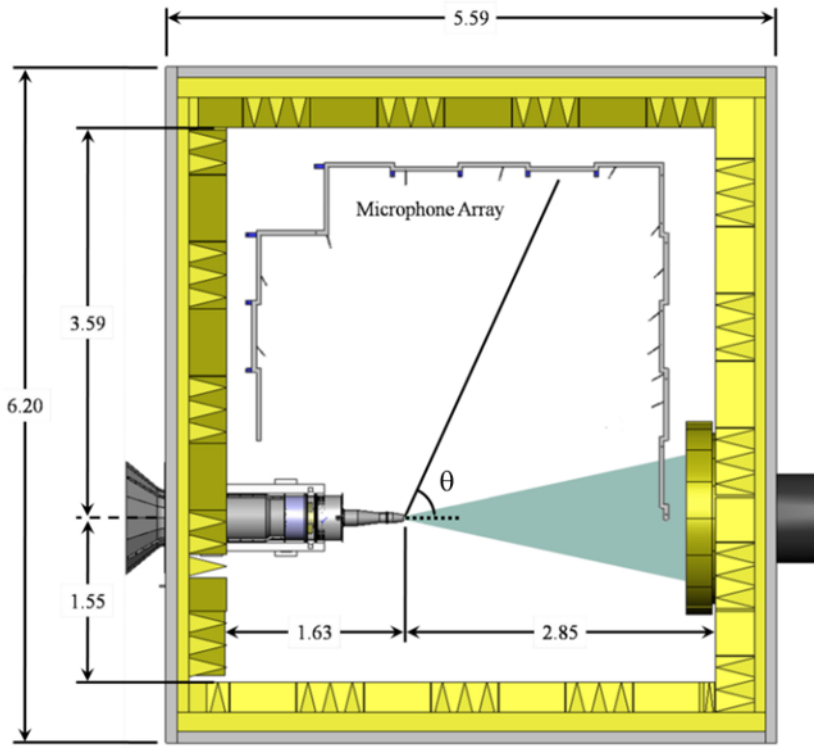

Figure 2.1: Top-down view of anechoic chamber and free jet facility at GDTL; dimensions are in meters.

for the LAFPA extension, which housed the eight actuators used in this study. For the experiments reported in this paper, the jet was operated at a Mach number (M_j) of 0.90, and with a total temperature ratio of approximately unity. The Reynolds number based on the jet exit diameter was 6.2×10^5; previous investigations using hot-wire anemometry have indicated that the initial shear layer is turbulent for this operating condition with momentum thickness 0.09 mm and boundary layer thickness 1 mm [Kearney?].

2.2 Localized Arc-Filament Plasma Actuators

2.3 Data Acquisition

2.3.1 Near- and Far-field Pressure

Near-field and far-field pressure measurements were acquired using Brel & Kjr inch 4939 microphones and preamplifiers. The signal from each microphone is band-pass filtered from 20 Hz to 100 kHz using a Brel & Kjr Nexus 2690 conditioning amplifier, and recorded using National Instruments PXI-6133 A/D boards and LabVIEW software. The microphones are calibrated using a Brel & Kjaer 114 dB, 1 kHz sine wave generator (model # ???). The frequency response of the microphones is flat up to roughly 80 kHz, with the protective grid covers removed.

Far-field acoustic pressure is acquired at three polar angles: 30, 60 and 90, as measured from the downstream jet axis. The positioning of the far-field microphone array can be seen in Fig. 2.1. The microphones were oriented such that they are at normal incidence to the jet downstream axis at the nozzle exit. The radial distance of the microphones ranges from 101D at 30 to 145D at 60.

The near-field pressure was acquired during two separate experimental campaigns; the first focusing purely on the near-field and far-field pressure and the second focusing on the instantaneous velocity field. During the first campaign, the irrotational near-field was acquired using a linear array of sixteen microphones located along the meridional plane of the jet; the spacing varied along the array from 1D to 2D Fig. 2.2. The array was mounted on an x-y linear traverse system the array and was inclined at an angle of 8.6 to the jet axis in order to match the spreading angle of the jet shear layer, as determined via PIV measurements during previous studies [28]. The traverse

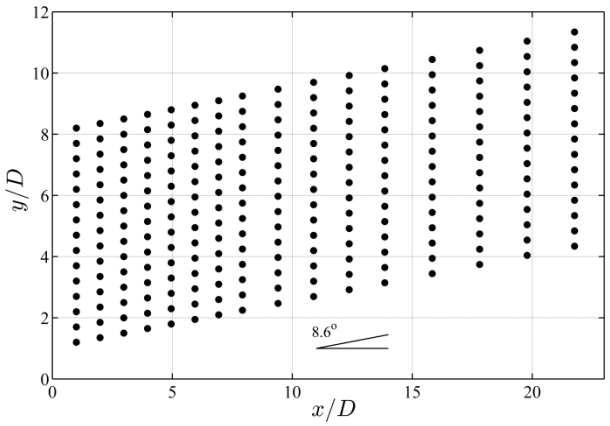

Figure 2.2: Schematic of the microphone positions ???

was controlled using LabView and enabled the acquisition of pressure measurements at various radial positions with respect to the jet axis. Initially, the most upstream microphone is positioned at x/D = 1 and r/D = 1.20, which is just outside the initial shear layer. For subsequent cases, the microphone array was incremented radially outward by 0.5D for a total travel distance of 7D, for a total of 15 array locations in the radial direction. Voltage signals were collected at 200 kHz with 81920 data points per block; sub-blocks of 8192 data points were used when calculating short-time power spectral densities, resulting in a frequency resolution of 24.4 Hz. Ten blocks were recorded for each case resulting in four seconds of data, which has been found to be sufficient for statistical convergence.

In the second experimental campaign, a shorter array consisting of 12 microphones equally space by $1D$ was used. In this case, the array was mounted from the floor and at an angle off the meridional plane of the jet (with microphone tips angled normal to the jet axis). This setup was used in conjunction with the particle image velocimetry described in the following section; the microphone array was placed off of

the meridional plane so that it did not intersect with the laser sheet. As before, the microphone array was angled 8.6 with respect to the jet axis in order to match the spreading rate of the shear layer, and the axial and radial position was set to match the closest microphone array location used during the first experimental campaign. Voltage traces were acquired at 400 kHz, with 24576 points collected per block.

2.3.2 Particle Image Velocimetry

The instantaneous velocity was acquired using streamwise, two-component particle image velocimetry (PIV). A Spectra Physics, double-pulsed Nd:YAG laser (model PIV-400) was used as the illumination source. Due to facility requirements, the laser was located on a vibrationally-damped table outside the anechoic chamber and the laser beam was routed into the chamber using an overhead port; this resulted in a beampath of $\sim$10 m. The laser sheet was formed using two cylindrical and one spherical lens; one of the cylindrical lenses was mounted to a rotational stage in order to ensure that the final laser sheet was normal to the jet exit (i.e. the laser sheet was streamwise to the jet). Alignment of the separate laser heads was initially performed using burn paper; final alignment was performed by seeding a low-velocity flow and visually checking that the same particles were captured in both frames. Per the best practices explained in the LaVision DaVis manual, the timing between the two laser pulses was set so that particles in the jet core translated downstream by roughly half of the minimum correlation window width (16 pixels). For the present work, this resulted in a time delay of 3 μs. It was later observed that the actual time delay produced by the laser did not match the delay specified in the control software; this resulted in incorrect velocities being computed by the cross-correlations. In order to

correct for this, the laser pulses were recorded using a ThorLabs DET210 photoreceiver and a LeCroy Wavejet ???? oscilloscope; the final vector fields were linearly scaled based on the ratio between the specified time delay and the measured time delay.

The jet core was seeded using Di-Ethyl-Hexyl-Sebacat (DEHS); the oil was atomized using a LaVision Aerosol generator and injected upstream of the turbulence screens in the stagnation chamber in order to produce a uniform seed particle density. As the jet entrains a significant amount of the surrounding ambient fluid as it evolves downstream, the coflow around the jet must also be seeded in order to accurately measure the outer shear layer velocity. For this, a TSI 6-jet atomizer (model 9306A) and olive oil was used; injection occurred into a plenum which surrounded the core stagnation chamber. Per the manufacturer's specfications, both atomizers provided nominally sub-micron seed particles. To ensure consistent seeding, this coflow was driven using a small blower (Model number???) and a series of high-pressure ejectors. As a result, for the PIV data acquisitions, the jet core was surrounded by a $\sim$5 m/s coflow.

Image groups were acquired using two LaVision Imager Pro SX 5M cameras. The cameras had 12-bit resolution and 2560$\times$2180 pixels. The combination of the PIV-400 laser and the Imager Pro SX cameras resulted in a maximum acquisition rate for the image groups of 5 Hz. Nikon Nikkor 105 mm f/1.8 lenses were used, and 532 nm bandpass filters were mounted on the lenses (what is the maker for the filters?!?!). The cameras were positioned such that they were nominally normal to the image plane, negating the need for scheimpflug mounts. This was done as having high spatial resolution and field of view were deemed to be more important than having

full, three-component velocity vectors. The cameras were aligned such that there was roughly a 10% overlap between the two images. This setup is generally designated as "side-to-side" in order to differentiate it from stereoscopic PIV. The cameras were calibrated simultaneously using a LaVision calibration plate (type 31). Hardware background subtraction was used in order to reduce the effect of reflections off of the nozzle extension and near-field microphone array.

The image groups were acquired in two modes: ensemble and phase-locked. When in phase-locked mode, a reference signal from the LAFPA control computer was used as an external trigger for LaVision's DaVis software; various filters were placed inline in order to damp the electromagnetic interference generated by the LAFPAs. The reference signal was downsampled to roughly 10 Hz by the LAFPA control computer, and delayed appropriately in time to control the acquired actuation phase. In ensemble mode, image groups were acquired randomly in time at the system's maximum acquisition rate (5 Hz). In this case, the PIV computer was set to output a reference signal which was used to trigger the acoustics data acquisition system. The timing was set such that the PIV image acquisition would occur roughly in the center of a data block acquired by the acoustics system; the signal from a ThorLabs DET210 photoreceiver was also recorded in order to accurately identify the timing of the image acquisition in relation to the pressure time traces.

Instantaneous velocity vectors were computed using LaVision's DaVis software. Multipass, FFT-based cross-correlations were used, with decreasing window size (64×64 for the initial pass, and 32×32 for the final three passes). A 50% overlap was used for the initial pass, and a 75% overlap was used for all subsequent passes. The velocity fields were post-processed to remove spurious vectors, which were iteratively replaced

if secondary correlation peaks were found, before the downstream and upstream images were combined. No interpolation, smoothing, or denoising was performed in post-processing.

Chapter 3: Near-field Signature of Aeroacoustic Sources

3.1 Preprocessing: Filtering the Actuator Self-Noise

Chapter 4: Stochastic Estimation of Time-resolved Velocity Fields

Chapter 5: Dilatation as the Aeroacoustic Acoustic Source

Chapter 6: Conclusions

Bibliography

[1] Marie Cabana, Vronique Fortun, and Peter Jordan. Identifying the radiating core of lighthill's source term. *Theoretical Computational Fluid Dynamics*, 22:87–106, 2008.

[2] P. Jordan and Y. Gervais. Subsonic jet aeroacoustics: associating experiment, modelling and simulations. *Experiments in Fluids*, 44:1–21, 2008.

[3] M. J. Lighthill. On sound generated aerodynamically. i. general theory. In *Proceedings of the Royal Society of London: Series A, Mathematical and Physical Sciences*, volume 211, pages 564–587. The Royal Society, 1952.

[4] Christopher K. W. Tam, Golebiowski, Michel, and J. M. Seiner. On the two components of turbulent mixing noise from supersonic jets. In *2nd AIAA/CEAS Aeroacoustics Conference*, volume AIAA Paper, 1996.

[5] Christopher K. W. Tam, K. Viswanathan, K. Ahuja, and J. Panda. The source of jet noise: Experimental evidence. *Journal of Fluid Mechanics*, 615:253–292, 2008.

[6] K Viswanathan. Scaling laws and a method for identifying components of jet noise. *AIAA Journal*, 44(10):2274–2285, 2006.